Hairy charged black holes
in a model with bounded scalar field potential

Yves Brihaye[1], Betti Hartmann [2], and Katherine Horton[2]

[1]Physique de l'Univers, Université de Mons, 7000 Mons, Belgium
[2]Department of Mathematics, University College London, Gower Street, London, WC1E 6BT, UK

April 3, 2025

Abstract

Electrically and magnetically charged (a.k.a. dyonic) black holes with scalar hair have recently been constructed for a sextic scalar field potential. Here, we re-investigate this model, but with a bounded scalar field potential of exponential form. We demonstrate that qualitative differences appear. First, we present scalar clouds on (dyonic) Reissner-Nordström black holes as well as (dyonically) charged clouds on Schwarzschild black holes, respectively. We then extend our results to the fully backreacted case and put the focus on the comparison of the electrically charged black holes with their dyonic counterparts.

1 Introduction

The no-scalar hair theorems [1] put restrictions on the existence of scalar hair on the horizon of a black hole. In an attempt to understand how high energy physics works in curved space-time, particle physics models involving scalar fields have been consider and it was shown that black holes with non-trivial scalar hair can exist. Examples of these are black holes that carry Skyrme hair [2] as well as Higgs hair [3]. In both of these cases, the flat space-time limit possesses topological soliton solutions, in the former case the Skyrmion [4], in the latter the 't Hooft-Polyakov magnetic monopole [5, 6]. Black holes with hair can then be thought of as residing in the center of these solitonic objects. Note that the SU(2) Yang-Mills-Higgs model does not only allow black holes inside monopoles, but also magnetically charged Reissner-Nordström solutions. The unbroken U(1) gauge field is associated to the long-range magnetic field. Boson stars are gravitating non-topological solitons [7, 8] that are made of a complex valued scalar field and possess a globally conserved Noether charge. That black holes cannot be put into the center of uncharged and non-rotating boson stars is due to the fact that the radial pressure associated to the scalar field is larger than the pressure in angular direction [9]. However, when either giving the solution angular momentum [10] and/or gauging the U(1) symmetry of the complex scalar field model [11, 12, 13] , black hole solutions with scalar hair can be constructed. A synchronisation condition has to be fulfilled which assigns either the horizon velocity or the electric potential at the horizon to the frequency of the complex scalar field, respectively. This condition appears exactly at the threshold of superradiance.

Recently, new types of spherically symmetric, static black holes which carry scalar hair were constructed [14]. These solutions possess both electric and magnetic fields with the magnetic field representing that of a magnetic monopole sitting at the origin of the coordinate system behind the event horizon. When magnetic fields are present, a complex doublet of scalar fields is necessary. This possesses a global $SU(2)$ symmetry and the dependence on the coordinates is such that the field equations remain cohomogeneity-one. The minimal coupling of the scalar field to the magnetic monopole charge requires the Dirac quantisation condition [15]. Accordingly, there exists no regular limit of the corresponding black hole solutions.

In this paper we follow the investigation of [14], but now choose a scalar field potential that is bounded. We discuss in detail the case of uncharged scalar fields in the background of an electrically and magnetically charged Reissner-Nordström black hole as well as electrically and magnetically charged scalar fields in the background of a Schwarzschild black hole, respectively. These limiting cases have not been investigated in detail before. We also discuss the electrically and magnetically charged black holes with scalar hair and compare our results to those obtained in [14], where a polynomial self-interacting scalar field potential was used.

We discuss the model in Section 2, scalar clouds on black holes in Section 3 and black holes with scalar hair in Section 4, respectively. We conclude in Section 5.

2   The model

The action of the model we are studying here reads:

$$\mathcal{S} = \int \mathrm{d}^4x\sqrt{-g}\left(\frac{\mathcal{R}}{4\alpha} + \mathcal{L}_m\right) \tag{1}$$

where $\alpha = 4\pi G$. This is the Einstein-Hilbert action with Ricci scalar $\mathcal{R}$ and Newton's constant G minimally coupled to matter fields with Lagrangian density $\mathcal{L}_m$. For the energy-momentum content we consider a number $n+1$ of self-interacting, massive and complex scalar fields Φ_k, $k = 1, ..., n+1$ minimally coupled to a U(1) gauge field A_μ with Lagrangian density

$$\mathcal{L}_m = \sum_{k=1}^{n+1}\left[-D_\mu\Phi_k(D^\mu\Phi_k)^* - U(\Phi_k\Phi_k^*)\right] - \frac{1}{4}F_{\mu\nu}F^{\mu\nu} \quad, \tag{2}$$

where $D_\mu = \partial_\mu - igA_\mu$ is the covariant derivative with gauge coupling g and $F_{\mu\nu} = \partial_\mu A_\nu - \partial_\nu A_\mu$ is the U(1) field strength tensor. In [14] this model was studied with a sextic potential, here we will use an exponential potential of the form :

$$U(\Phi_k\Phi_k^*) = m^2\eta^2\left(1 - \exp(-\Phi_k\Phi_k^*/\eta^2)\right) \tag{3}$$

where η is an energy scale. Note that unlike the sextic potential used in [14] this potential is bounded in $|\Phi|$.

2.1   The Ansatz and equations of motion

In the following, we will study spherically symmetric solutions and hence use the Ansatz

$$\mathrm{d}s^2 = -N(r)\sigma^2(r)\mathrm{d}t^2 + \frac{1}{N(r)}\mathrm{d}r^2 + r^2\mathrm{d}\theta^2 + r^2\sin^2\theta\mathrm{d}\varphi^2 \quad, \quad N(r) = 1 - \frac{2\mu(r)}{r} \tag{4}$$

for the metric with $\mu(r)$ the mass function and [14]

$$A_\mu\mathrm{d}x^\mu = V(r)\mathrm{d}t + Q_m\cos(\theta)\mathrm{d}\varphi \tag{5}$$

for the U(1) gauge field. The parameter Q_m denotes the magnetic charge of the solution. For the scalar field, we distinguish the cases $k = 0$ and $k = 1$, where $k \in \mathbb{N}$ appears in the Dirac quantisation condition $(c = \hbar = 1)$:

$$gQ_m = \pm\frac{k}{2} \quad, \quad k \in \mathbb{N} \ . \tag{6}$$

The electric and magnetic fields of the solutions is given by

$$E_r = -F_{r0} = -\frac{\mathrm{d}V}{\mathrm{d}r} \quad, \quad B_r = \frac{F^{\theta\varphi}}{\sqrt{-g}} = -\frac{Q_m}{r^2} \quad, \tag{7}$$

where the latter describes the field of a magnetic monopole located at the origin. In the following, the choice of Ansatz for the scalar field depends on whether we choose $Q_m = 0$ or $Q_m \neq 0$. For $k = 0$, i.e. scalar fields charged only electrically, we choose

$$\Phi = \phi(r)e^{-i\omega t} \tag{8}$$

and for $k = 1$, i.e. electrically and magnetically charged scalar fields, we choose [14]

$$\Phi_1 = \phi(r)\sin\left(\frac{\theta}{2}\right)e^{i(\varphi/2 - \omega t)} \quad , \quad \Phi_2 = \phi(r)\cos\left(\frac{\theta}{2}\right)e^{-i(\varphi/2 + \omega t)} \tag{9}$$

The equations of motion that result from the variation of (1) are invariant under the following rescaling of the fields and coupling constants

$$\phi \to \frac{\phi}{\eta} \quad , \quad r \to mr \quad , \quad V \to \frac{V}{\eta} \quad , \quad Q_m \to \frac{m}{\eta}Q_m \quad , \quad g \to \frac{\eta}{m}g \quad , \tag{10}$$

which, in particular, leaves the Dirac quantization invariant. We will use these rescalings to set the scalar field mass $m = 1$, $\eta = 1$ without loss of generality. With this choice, the field equations read :

$$\mu' = \alpha\left[r^2 N\phi'^2 + \frac{r^2 g^2 V^2 \phi^2}{\sigma^2 N} + \frac{k}{2}\phi^2 + \frac{r^2 V'^2}{2\sigma^2} + \frac{k^2}{8g^2 r^2} + r^2\left(1 - \exp(-\phi^2)\right)\right] , \tag{11}$$

$$\frac{\sigma'}{\sigma} = 2\alpha r\left[\phi'^2 + \frac{g^2 V^2 \phi^2}{\sigma^2 N^2}\right] , \tag{12}$$

$$\left(\frac{r^2 V'}{\sigma}\right)' = 2\frac{r^2 g^2 V\phi^2}{\sigma N} , \tag{13}$$

$$\left(\sigma r^2 N\phi'\right)' = -\frac{r^2 g^2 V^2 \phi}{\sigma N} + \frac{k}{2}\sigma\phi + r^2\sigma\phi\exp(-\phi^2) . \tag{14}$$

Note that the synchronisation condition for black holes with scalar hair reads $\omega = gV_h$, where $V_h = V(r_h)$ is the value of the electric potential on the horizon r_h and we have chosen $\omega = V_h = 0$ in the equations above. Also note that the effective mass of the scalar field is given by

$$m_{\text{eff}}^2 := m^2 - g^2 V_\infty^2 \tag{15}$$

where V_∞ is the value of the gauge field $V(r)$ at $r \to \infty$. We also require $m_{\text{eff}}^2 \geq 0$ which ensures that the scalar field is exponentially localised. Since $V(r_h) = 0$, the value of V_∞ determines the potential difference between the horizon and infinity. Requiring $m^2 \geq g^2 V_\infty^2$ then means that we cannot choose g and/or V_∞ too large, otherwise, we would be able to create scalar particles of mass m.

The model possesses a U(1) symmetry that leads to the conserved Noether charge

$$Q_N = \int_{r_h}^{\infty} dr\; r^2 \frac{2gV\phi^2}{N\sigma} . \tag{16}$$

The Noether charge Q_N can be thought of as the number of scalar bosons making up the cloud that surrounds the black hole horizon. Due to the coupling to the electromagnetic field, these scalar bosons possess each an electric charge g, such that the electric charge in the scalar cloud is gQ_N. When the matter fields are not coupled to the gravitational fields, we define the mass M_Q of the cloud as

$$M_Q = \frac{1}{4\pi}\int d^3x \;\sqrt{-g}\left(T_i^i - T_0^0\right) . \tag{17}$$

In the following, we will also use the ADM mass M_{ADM} for the fully back-reacted case, where $M_{\text{ADM}} = \mu(r \to \infty)$. Finally, the Hawking temperature of the black holes reads

$$T_H = \frac{1}{4\pi}\sigma(r_h)N'(r)|_{r=r_h} . \tag{18}$$

3

3 Scalar clouds on black holes

The scalar field not back-reacting on the space-time is an interesting limit that has not been investigated in detail in [14] or anywhere else in the literature. We will close this gap here and discuss two cases separately: (a) the scalar field equation decoupled from the Einstein-Maxwell equations, and (b) both matter fields (scalar and electromagnetic) decoupled from gravity. In the former case this leads to the study of scalar fields in the background of (dyonic) Reissner-Nordström solutions, while in the latter case, the background is the Schwarzschild solution and the scalar field is electrically (and magnetically) charged.

3.1 Scalar clouds on (dyonic) Reissner-Nordström black holes

In order to decouple the scalar field from the Einstein-Maxwell equations we rescale $V \to V/\sqrt{\alpha}$ and $g \to \sqrt{\alpha} g$ and let $\alpha = 0$. The solution to the Einstein-Maxwell equations is the electrically (and magnetically) charged Reissner-Nordström (RN) solution with metric functions :

$$\sigma(r) \equiv 1 \quad , \quad N = 1 - \frac{2M_{\mathrm{ADM}}}{r} + \frac{(Q_e^2 + Q_m^2)}{r^2} = \frac{(r - r_+)(r - r_-)}{r^2} \tag{19}$$

with the two horizons $r_{\pm} = 2M_{\mathrm{ADM}} \pm \sqrt{M_{\mathrm{ADM}}^2 - (Q_e^2 + Q_m^2)}$. Q_e denotes the electric charge, while $Q_m = \pm k/(2g)$ is the magnetic charge. The mass M_{ADM} can be written in terms of the event horizon radius $r_+ = r_h$ and the charges as follows

$$M_{\mathrm{ADM}} = \frac{r_h}{2} \left(1 + \frac{\left(Q_e^2 + \frac{k^2}{4g^2} \right)}{r_h^2} \right) \quad . \tag{20}$$

The electric potential for this solution is then

$$V(r) = Q_e \left(\frac{1}{r_h} - \frac{1}{r} \right) = V_{\infty} - \frac{Q_e}{r} \tag{21}$$

where we have defined the value of the electric potential at infinity $V_{\infty} := Q_e/r_h$. The remaining equation to be solved is the scalar field equation (14) subject to appropriate boundary conditions. Requiring regular scalar fields on the horizon $r = r_h$ leads to :

$$(N'\phi')|_{r=r_h} = \frac{1}{2} \frac{dU}{d\phi} \bigg|_{r=r_h} + \frac{k\phi(r_h)}{2r_h^2} \quad . \tag{22}$$

For the effective mass (15) we find in this case

$$m_{\mathrm{eff}}^2 = m^2 - \frac{g^2 Q_e^2}{r_h^2} \quad . \tag{23}$$

This leads to an upper bound on the value of g. Moreover, it is well known that extremal black holes cannot carry scalar hair. Hence, we also need to require that $M_{\mathrm{ADM}}^2 > Q_e^2 + Q_m^2$, which leads to a lower bound on g. Combining these two bounds, we find :

$$\frac{k}{2} \sqrt{\frac{1}{r_h^2 - Q_e^2}} < g < \frac{m r_h}{Q_e} \quad . \tag{24}$$

Note that in the following, as stated above, $m = 1$ without loss of generality.

3.1.1 Scalar clouds on electrically charged RN black holes

We first discuss the case $k = 0$, i.e. a scalar field in the background of an electrically charged RN black hole. The scalar field equation (14) needs to be solved numerically. Fixing $r_h = 1.0$ and Q_e to different values, our numerical results strongly suggest that scalar clouds exist for $g \in g \in]0, g_{\max}]$ with $g_{\max} = \frac{mr_h}{Q_e}$ in agreement with (24). In the limit $g \to g_{\max}$ we find that both $\phi(r_h) \to 0$ and $m_{\text{eff}}^2 \to 0$, i.e. the scalar field function becomes equivalent to the null function. For g decreasing, on the other hand, the value of the scalar field on the horizon, $\phi(r_h)$, increases. The dependence of gQ_e and m_{eff}^2 on the parameter $\phi(r_h)$ is qualitatively and quantitatively practically unchanged when considering different values of Q_e.

3.1.2 Scalar clouds on electrically and magnetically charged RN black holes

We now turn to the case $k = 1$. We show the scalar field function $\phi(r)$ for clouds on electrically and magnetically charged RN black holes with $r_h = 1.0$ and $Q_e = 0.12$ in Fig. 1 (left). A general feature of these solutions is that the scalar field develops a local maximum at some intermediate radius. We find that increasing g and hence decreasing the magnetic charge Q_m of the background RN solution that the value of the local maximum of $\phi(r)$ decreases and is located at decreased values of the radial coordinate r. To understand the difference to the $k = 0$ case, we show the profiles of $\phi(r)$ and $\phi'(r)$ in Fig. 1 (right) for $r_h = 1.0$, $Q_e = 0.12$, $g = 1.0$ and compare the cases $k = 0$ and $k = 1$. Clearly, for the same value of the horizon radius and the same value of the gauge coupling g, scalar clouds on electrically charge RN black holes are qualitatively different to scalar clouds on electrically and magnetically charged RN black holes: the scalar field has larger values on the horizon and the clouds extend to smaller radii in the former case. The presence of the magnetic charge seems to push the scalar cloud away from the horizon.
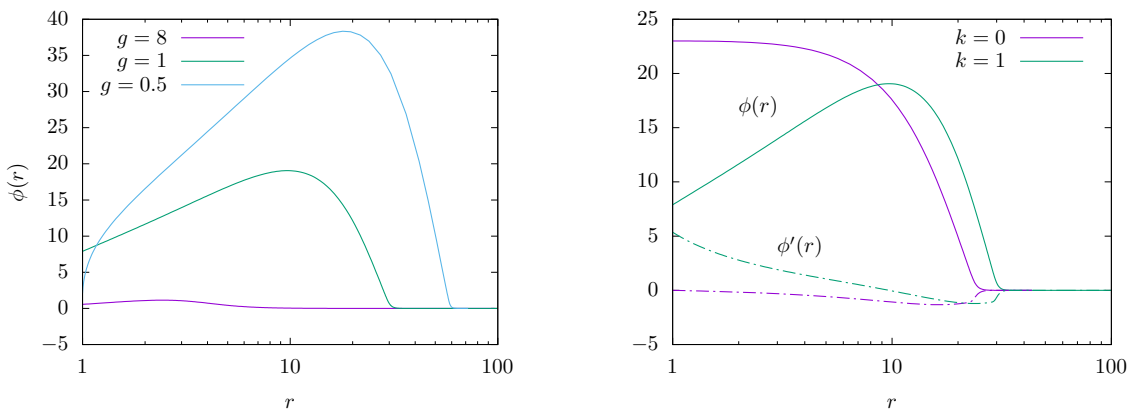

Figure 1: *Left*: We show the scalar field function ϕ for clouds on electrically and magnetically charged RN black holes with $r_h = 1.0$, $Q_e = 0.12$, $n = 1$ and three different values of the gauge coupling g. Note that different values of g correspond to different magnetic charges Q_m of the RN solutions, $Q_m = 1/(2g)$. *Right*: We show the profile of $\phi(r)$ as well as of $\phi'(r)$ for scalar clouds on RN black holes with $r_h = 1.0$, $Q_e = 0.12$, $g = 1.0$ and two different values of k. Note that for $k = 0$ the RN black hole is only electrically charged, while for $k = 1$, the RN black hole possesses additionally a magnetic charge $Q_m = 0.5$.

Our numerical results also confirm the validity of (24), i.e. the fact that for scalar clouds to exist on electrically and magnetically charged RN black holes g cannot be arbitrarily small. The interval of g for which non-trivial scalar field solutions exist, becomes smaller when either decreasing r_h or increasing Q_e. In

Fig. 2 we show the dependence of gQ_e, m_{eff}^2, $\phi'(r_h)$ on $\phi(r_h)$ (left) as well as the dependence of M_Q and Q_N on gV_∞ (right) for $r_h = 1.0$ and $Q_e = 0.12$. The comparison of the $k = 0$ and $k = 1$ demonstrates that while we find only one branch of solutions in $\phi(r_h)$ when $k = 0$, we find two branches when $k = 1$. Moreover, these two branches join at a maximal value of $\phi(r_h)$, while $\phi(r_h)$ can tend to infinity for $k = 0$. One branch terminates at $m_{\text{eff}}^2 = 0$ (similar to the $k = 0$ case), the second branch bifurcates with the extremal RN solution. Our numerical results confirm that this limit is reached for $g \approx 0.503$ which is in perfect agreement with (24). Extremal RN black holes cannot carry regular scalar hair and hence we find that $\phi'(r_h) \to \infty$ in this limit. In Fig. 2 (right) we show the dependence of the mass M_Q and the Noether charge Q_N on gV_∞. We find only one branch of solutions for both $k = 0$ and $k = 1$ and that both the mass M_Q and the Noether charge Q_N tend to finite values in the limit $gV_\infty \to 1$. On the other hand, M_Q and Q_N diverge for $gV_\infty \to 0$. The clouds on electrically charged RN black holes have lower values of M_Q and Q_N than their counterparts on electrically and magnetically charged RN black holes. For both $k = 0$ and $k = 1$ we find that the Noether charge is larger than the mass M_Q.
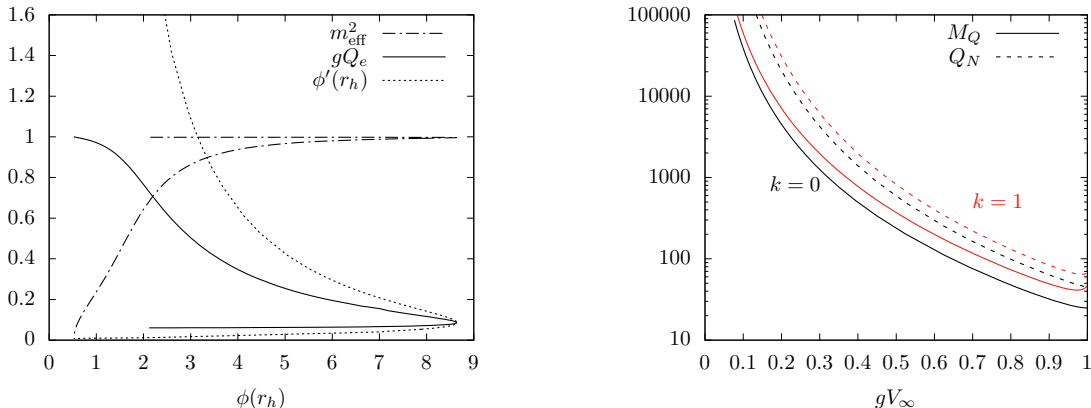

Figure 2: *Left*: We show the dependence of m_{eff}^2 (dotted-dashed), gQ_e (solid) and $\phi'(r_h)$ (dotted) on $\phi(r_h)$ for scalar clouds on RN black holes with $r_h = 1$, $Q_e = 0.12$ and $k = 1$. *Right*: We show the dependence of the mass M (solid) and the Noether charge Q_N (dashed) on gV_∞ for scalar clouds on RN black holes with $r_h = 1$ and $Q_e = 0.12$. We compare the $k = 0$ (black) and $k = 1$ (red) case.

3.2 Charged scalar clouds on Schwarzschild black holes

Another interesting limiting case is $\alpha = 0$, i.e. the limit in which all matter fields decouple from gravity. The unique solution to the vacuum Einstein equation is the Schwarzschild space-time with $N(r) = 1 - r_h/r$, $\sigma(r) \equiv 1$. This solution is uniquely characterized by the event horizon r_h.

3.3 Electrically charged clouds on Schwarzschild black holes

Let us first discuss the case $k = 0$. We find that non-trivial scalar fields exist for $g \in]0, g_{\text{max}}]$ and that g_{max} depends on the event horizon radius r_h, e.g. $g_{\text{max}} \approx 0.11$ for $r_h = 0.15$, while $g_{\text{max}} \approx 0.05$ for $r_h = 1.0$, i.e. larger (and more massive) Schwarzschild black holes require smaller values of the gauge coupling g. The solutions can be characterized uniquely by the value of the electric field on the horizon $\sim V'(r_h)$ and exist for $V'(r_h) \in [W_1, W_2]$ where $W_{1,2}$ depend on g and r_h. For $g \to g_{\text{max}}$ we find that $W_1 \to W_2$. In the two limits $V'(r_h) \to W_{1,2}$ the effective mass of the scalar field, $m^2 - g^2 V_\infty^2$, tends to zero, i.e. the scalar field is

no longer exponentially localized. In the Table 1 we give the values of the minimal and maximal value of the electric field on the horizon for $r_h = 0.15$ and different values of g. Obviously, charged scalar clouds exist on Schwarzschild black holes only when the electric field is sufficiently large and at the same time not too large. Clearly, the electric field is necessary to allow for scalar clouds to exist on Schwarzschild black holes.

g	W_1	W_2
0.01	0.8	660.0
0.02	4.2	330.0
0.08	22.0	78.0
0.10	27.0	59.0
0.11	45.0	45.0

Table 1: The minimal (W_1) and maximal (W_2) value of the electric field $V'(r_h)$ of a scalar cloud on the horizon of a Schwarzschild black hole with $r_h = 0.15$.

In Fig. 3 we give the value of the scalar field on the horizon, $\phi(r_h)$, (left) and the electric charge Q_e (right) of the scalar cloud in dependence of gV_∞. Clearly, who branches appear in gV_∞ which both end at $gV_\infty = 1$ and merge at a minimal value of gV_∞. This minimal value of gV_∞ corresponds to an intermediate value of the electric field on the horizon, $V'(r_h)$. The lower branch in $\phi(r_h)$ corresponds to larger values of the electric field on the horizon, $V'(r_h)$, while the upper branch has lower values of the electric field on the horizon. Similarly, the lower branch in Q_e corresponds to larger values of $V'(r_h)$, while the upper branch corresponds to smaller values of $V'(r_h)$. Hence, electrically charged scalar clouds on Schwarzschild black holes have either small values of the scalar field on the horizon with large electric fields and small electric charge of the cloud, or they have large scalar fields with small electric fields and large electric charge of the cloud.
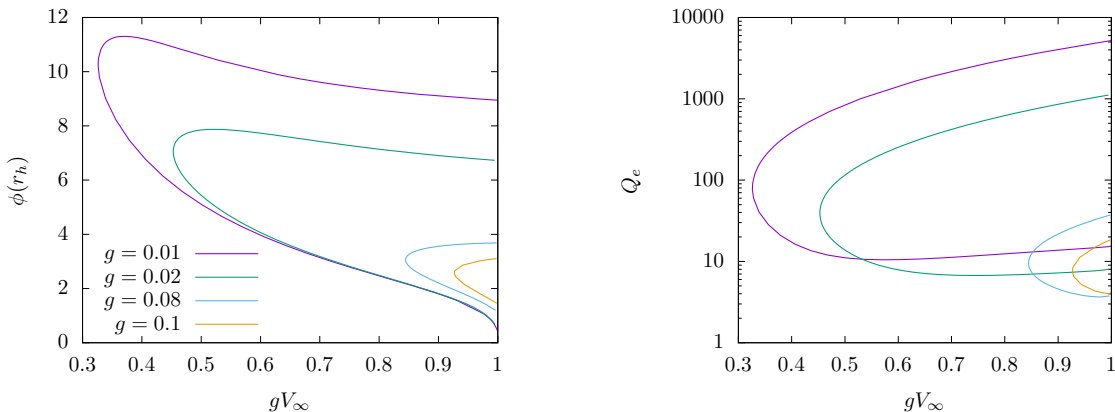

Figure 3: *Left*: We show the dependence of the scalar field on the horizon, $\phi(r_h)$, on gV_∞ for electric clouds on Schwarzschild black holes with $r_h = 0.15$ and several values of g. *Right*: Same as left, but for the electric charge Q_e of the scalar cloud.
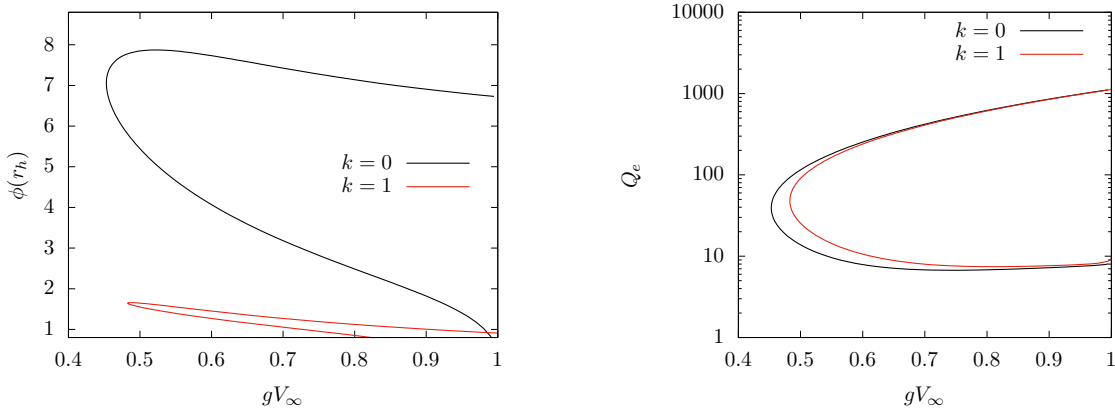
Figure 4: *Left* : We show the value of the scalar field on the horizon $\phi(r_h)$ in dependence of gV_∞ for electric ($k = 0$, black) and dyonic ($k = 1$, red) clouds on Schwarzschild black holes with $r_h = 0.15$ and $g = 0.02$. *Right* : Same as left, but for the electric charge of the scalar cloud Q_e.

3.3.1 Electrically and magnetically charged clouds on Schwarzschild black holes

Setting $k = 1$, we study electrically and magnetically charged scalar clouds on Schwarzschild black holes. In order to understand the influence of the magnetic charge on the solutions, we compare the cases $k = 0$ and $k = 1$ in Fig. 4, where we give the scalar field on the horizon $\phi(r_h)$ (left) and the electric charge of the scalar cloud Q_e (right) in dependence of gV_∞ for $g = 0.02$ and $r_h = 0.15$. Again, we find two branches of solutions in gV_∞ which both end at $gV_\infty = 1$ and join at a minimal value of gV_∞. This minimal value is slightly smaller for $k = 0$ solutions as compared to $k = 1$ solutions. While the additional magnetic charge does not change the value of Q_e strongly, the value of the scalar field on the horizon $\phi(r_h)$ is much smaller for $k = 1$ as compared to $k = 0$ solutions. Electrically charged scalar fields can possess much larger values on the event horizon of a Schwarzschild black hole as electrically and magnetically charged scalar fields.

4 Charged black holes with scalar hair

In the fully backreacted case, we are left with three free parameters after appropriate rescaling of the coordinate and fields, respectively. These are the gravitational coupling α, the gauge coupling g and the radius of the event horizon of the black hole r_h. We find that for a fixed choice of α, g and r_h a family of solutions can be constructed by using the value of the electric field on the horizon, $V'(r_h)$, or, alternatively, the value of the scalar field on the horizon, $\phi(r_h)$. We find several branches in these parameters. First, let us give the relation between these two parameters. This is shown in Fig. 5, where we compare the purely electric case (left, $k = 0$) with the dyonic case (right, $k = 1$). Clearly, the pattern is qualitatively very different for the two cases, in particular, the value of the scalar field on the horizon, $\phi(r_h)$ can be much larger for electrically charged black holes as compared to dyonic black holes.

In the $k = 0$ case, we find that for sufficiently small values of g two branches exist, labeled A and B in Fig. 5 (left). The solutions on these two branches are very different. This is shown in Fig. 6, where we give the profiles of the metric function $N(r)$ and $\sigma(r)$ as well as the electric field $V'(r)$ and the scalar field $\phi(r)$, respectively, for a solution on the branch A (left) and for a solution on the branch B (right) for $g = 0.01$ and $r_h = 1.0$. The solution from branch A has a small electric field on the horizon, $V'(r_h) = 0.1$, and clearly shows a hard wall at $r_c > r_h$ such that for $r > r_c$ the solution corresponds to an extremal RN

8

solution with vanishing scalar field $\phi(r) \equiv 0$, while for $r < r_c$ the scalar field is constant, but non-vanishing. As was discussed previously in [16, 17, 18], the interior of this solution can be interpreted as inflating with the constant scalar field energy equal to the positive cosmological constant. On the other hand, the solution on branch B has a large electric field on the horizon, $V'(r_h) = 2.0$. The scalar field becomes identically zero for large enough r at $r = r_c$ such that for $r > r_c$ the solution is given by $\phi \equiv 0$, $\sigma \equiv 1$, while $N(r)$ and $V'(r)$ are non-trivial and, in particular, $N(r_c) > 0$.
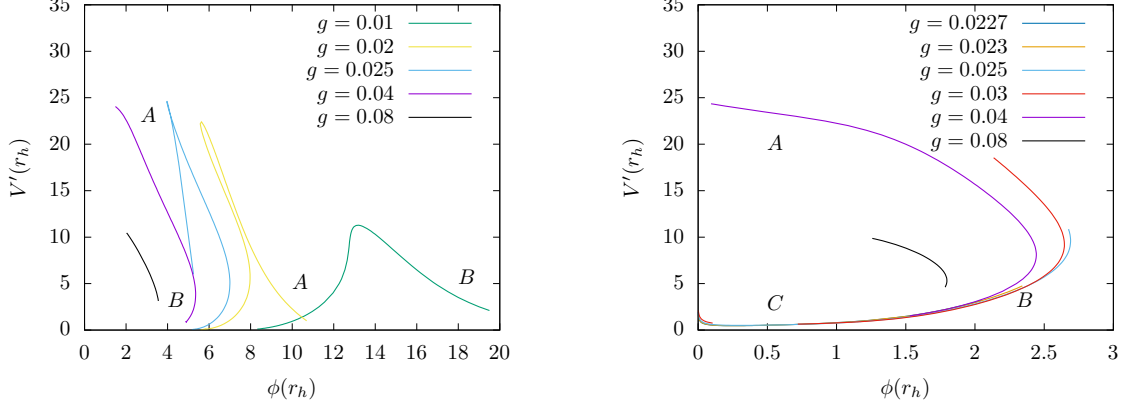
Figure 5: *Left* : We show the dependence of the value of the electric field on the horizon, $V'(r_h)$, on the value of the scalar field on the horizon, $\phi(r_h)$ for electrically charged black holes ($k = 0$) with scalar hair for $\alpha = 0.01$, $r_h = 1.0$ and several values of the gauge coupling g. *Right* : Same as left, but for electrically and magnetically charged, i.e. dyonic black holes ($k = 1$).
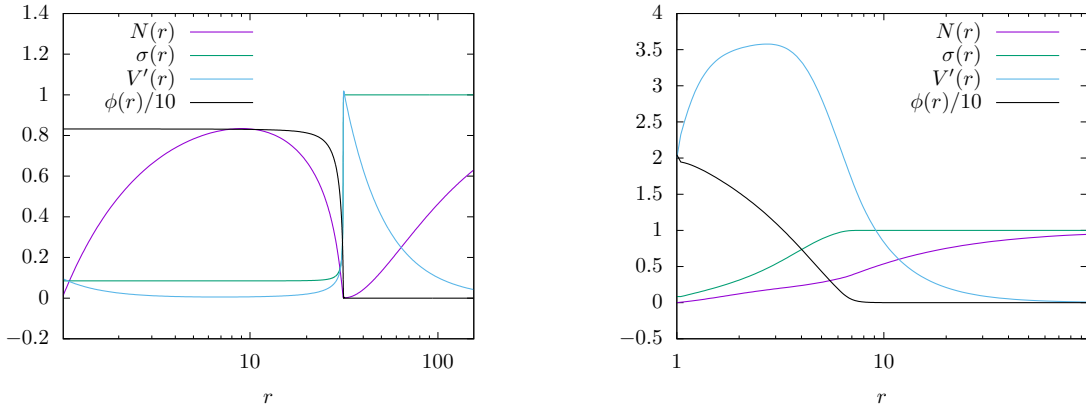

Figure 6: *Left* : We show the profile of the metric function N, of the electric field V', and the scalar field ϕ for the solution on branch A (see Fig.5) with $g = 0.01$ and $V'(r_h) = 0.1$. *Right* : Same as left, but for the solution on branch B with $g = 0.01$ and $V'(r_h) = 2.0$.

For the $k = 1$ solutions, we find a third branch (labeled C in Fig. 5) for intermediate values of g. In

order to understand this new branch, we show the profiles of solutions for $r_h = 1.0$, $\alpha = 0.001$, $g = 0.03$ in Fig. 7. On the left of this figure a solution for $\phi(r_h) = 2.0$ which corresponds to the merging point of branches A and B in Fig. 5 (right, red line) is shown. The scalar field becomes identically zero for $r > r_c$ and the electric field corresponds to that of RN solution. For $r_h < r < r_c$, the solution is non-trivial and, in particular, the scalar field does no longer have its maximal value at r_h. The scalar cloud is pushed away from the horizon when adding magnetic charge. On the right of Fig. 7 we show a solution on branch C. This solution has very small scalar field and $\sigma = \sigma_0 = \text{constant} < 1$ on and outside the horizon up to some intermediate value of $r = r_0$. For $r > r_0$ and $r < r_c$, the scalar field (and with it the remaining matter and metric functions) are non-trivial, while for $r > r_c$, we find $\phi(r) \equiv 0$, $\sigma \equiv 1$, the electric field becomes equal to that of a RN solution, $V' = V'_{RN}$, while $N(r)$ possesses a minimum. Our numerical results suggest that for the values of coupling constants chosen here, the minimum actually never drops down to zero. Hence, in contrast to the electric case, we do not find "hard wall" solutions with an inflating interior, but rather a solution that has different behaviour on the intervals $r \in [r_h, r_0]$, $[r_0, r_c]$ and $[r_c, \infty[$. The solution for $[r_c, \infty[$ is an extremal RN solution, while the solution in $[r_0, r_c]$ is non-trivial. The solution for $r \in [r_h, r_0]$ is given by

$$V(r) = V_\infty + \frac{Q_e}{r} \quad , \quad N(r) = 1 - \frac{2M_{\text{ADM}}}{r} + \frac{\alpha Q_e^2}{\sigma_0^2 r^2} + \frac{\alpha k^2}{4g^2 r^2} \quad . \tag{25}$$

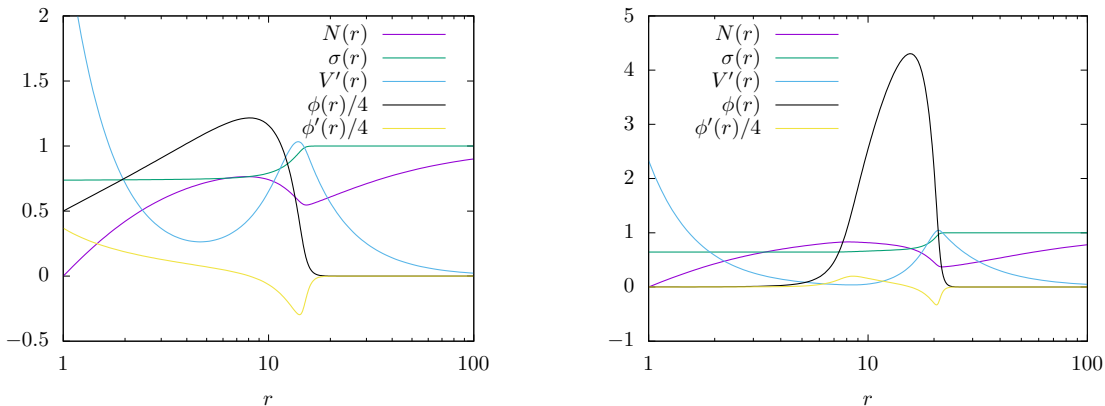Note that the electric charge is modified by a factor of $1/\sigma_0$ in $N(r)$.

Figure 7: *Left:* We show the profiles of the metric functions $N(r)$ and $\sigma(r)$, the electric field $V'(r)$, the scalar field $\phi(r)$ and the scalar field derivative $\phi'(r)$ for a dyonic black hole with $r_h = 1.0$, $\alpha = 0.001$, $g = 0.03$ and $\phi(r_h) = 2.0$. *Right:* We show the profiles of the metric functions $N(r)$ and $\sigma(r)$, the electric field $V'(r)$, the scalar field $\phi(r)$ and the scalar field derivative $\phi'(r)$ for a dyonic black hole with $r_h = 1.0$, $\alpha = 0.001$, $g = 0.03$ and $\phi(r_h) = 0.0002$.

In Fig. 8, we show the ADM mass of the solutions, M_{ADM}, in dependence of gV_∞ for $\alpha = 0.01$, $r_h = 1.0$ and several values of g. We compare the $k = 0$ (left) and the $k = 1$ (right) case. We find that for large values of g, the electrically charged and the dyonic black holes show the same pattern : there exist two branches of solutions which both terminate at $gV_\infty = 1$. These branches are labeled A and B in the plot.

For lower values of the gauge coupling g branch C appears here as well. Interestingly, some of these branches terminate at intermediate values of gV_∞, i.e. at $gV_\infty < 1$. Our numerical results indicate that the qualitative features of these new branches differ when comparing $k = 0$ and $k = 1$. To understand these features, it is instructive to compare the values of the Hawking temperature T_H. This is shown in Fig. 9.

We find that for $g > 0.04$, all solutions have non-zero temperature and the solutions with lowest ADM mass have also the lowest temperature T_H. However, our numerical results strongly suggest that for $g < 0.04$ we find solutions with $T_H \to 0$. However, due to limited numerical accuracy, we can only rely on our results for $T_H \gtrsim 10^{-3}$.
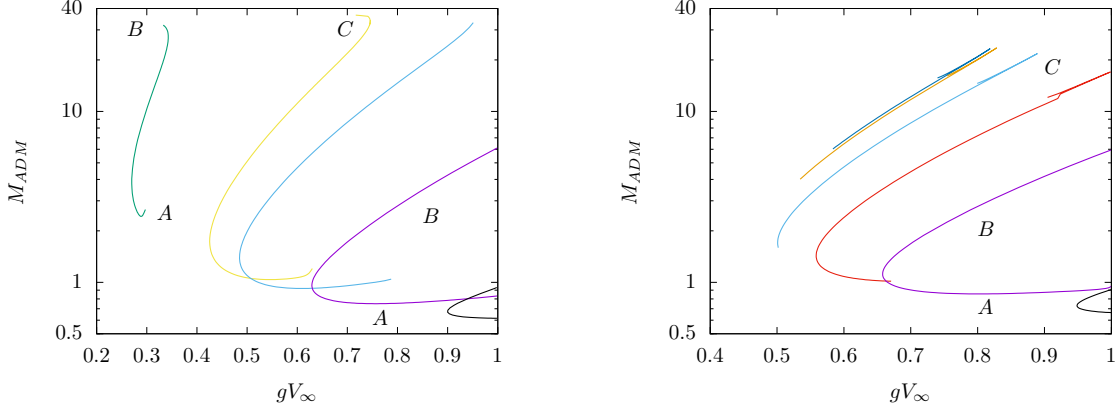

Figure 8: We show the dependence of the ADM mass M_{ADM} on gV_∞ for $\alpha = 0.01$, $r_h = 1.0$ and several values of g - colour-coding as in Fig. 5. We compare the purely electric case $k = 0$ (left) with the dyonic case $k = 1$ (right).
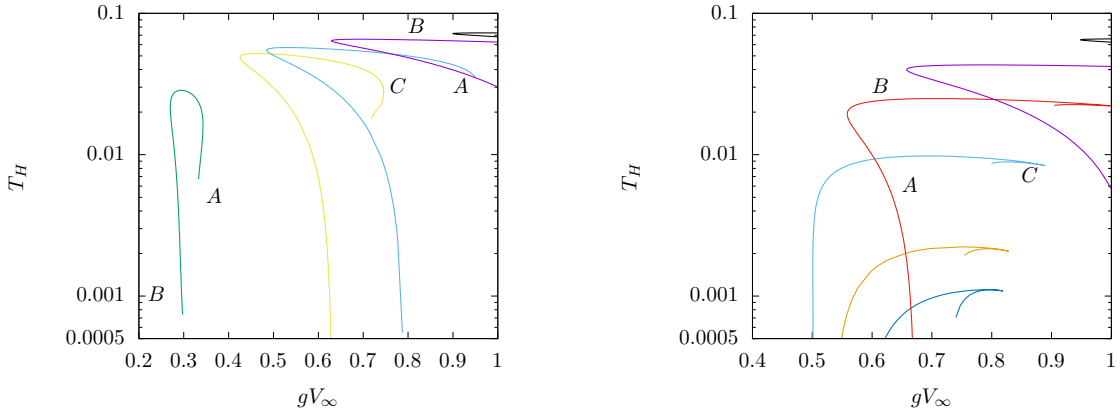

Figure 9: We show the dependence of the Hawking temperature T_H on gV_∞ for $\alpha = 0.01$, $r_h = 1.0$ and several values of g - colour-coding as in Fig. 5. We compare the purely electric case $k = 0$ (left) with the dyonic case $k = 1$ (right).

In Fig. 10 we show the value of the scalar field on the horizon, $\phi(r_h)$, in function of gV_∞ for $\alpha = 0.01$ and $r_h = 1.0$ and several values of g. We note that the presence of the magnetic charge allows for solutions with $\phi(r_h) \approx 0$. In the electric case, $\phi(r_h) = 0$ would imply $\phi(r) \equiv 0$, however, since the presence of the magnetic charge leads to a maximal value of $\phi(r)$ away from the horizon $\phi(r_h) \approx 0$ does not imply a trivial
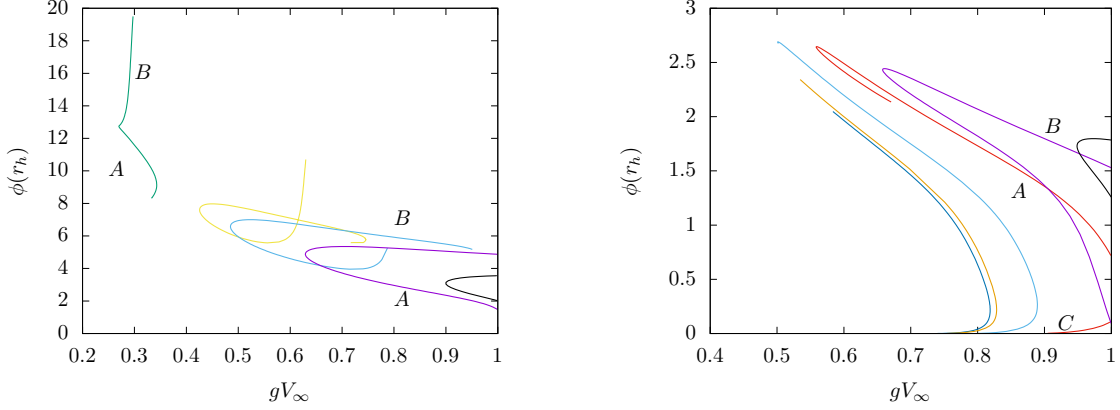
11

Figure 10: We show the dependence of the value of the scalar field on the horizon, $\phi(r_h)$, on gV_∞ for $\alpha = 0.01$, $r_h = 1.0$ and several values of g - colour-coding as in Fig. 5. We compare the purely electric case $k = 0$ (left) with the dyonic case $k = 1$ (right).

scalar field in the dyonic case. Close to $\phi(r_h) = 0$, we observe the existence of branch C. This branch can also be seen in Fig. 11. It corresponds not only to very small scalar fields at r_h, but also to increased electric fields on the horizon and decreased potential difference between the horizon and infinity when compared to branch B.
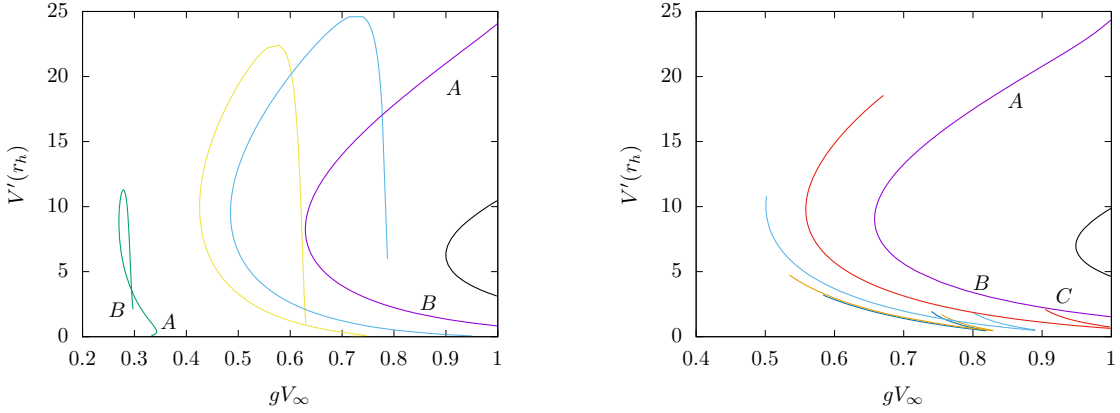

Figure 11: We show the dependence of the value of the electric field on the horizon, $V'(r_h)$, on gV_∞ for $\alpha = 0.01$, $r_h = 1.0$ and several values of g - colour-coding as in Fig. 5. We compare the purely electric case $k = 0$ (left) with the dyonic case $k = 1$ (right).

Let us finally note that the emergence of branch C for $g \approx 0.03$ came as a surprise. To understand this branch C better, we show the dependence of the value of the electric field on the horizon, $V'(r_h)$, on the value of the scalar field on the horizon, $\phi(r_h)$, for $\alpha = 0.01$, $r_h = 1.0$ and three values of g close to $g = 0.03$ in Fig. 12 (left). The new branch appears for sufficiently small values of $\phi(r_h)$ and corresponds to small values
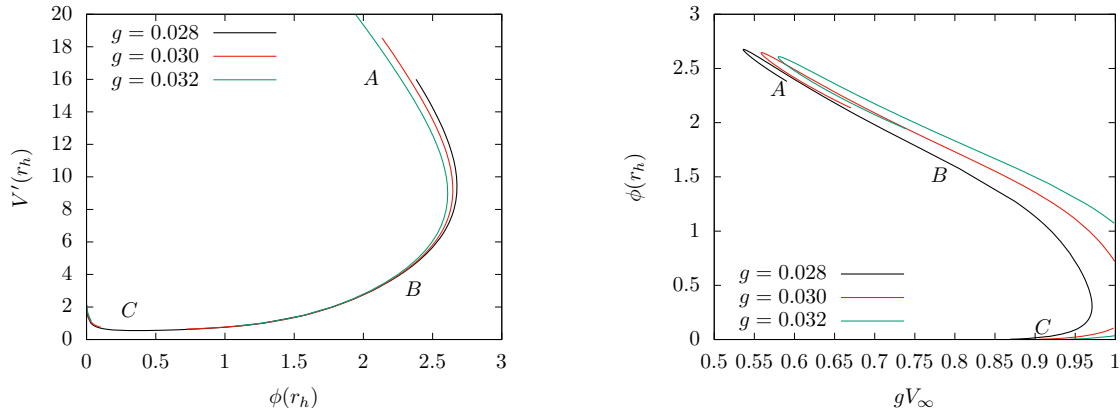
Figure 12: *Left:* We show the dependence of the value of the electric field on the horizon, $V'(r_h)$, on the value of the scalar field on the horizon, $\phi(r_h)$, for $\alpha = 0.01$, $r_h = 1.0$ and three values of g close to $g = 0.03$. *Right:* We show the dependence of the value of the value of the scalar field on the horizon, $\phi(r_h)$, on gV_∞ for $\alpha = 0.01$, $r_h = 1.0$ and three values of g close to $g = 0.03$.

of the electric field on the horizon. The dependence of $\phi(r_h)$ on gV_∞ show in the same figure on the right demonstrates that the limitation of $gV_\infty \leq 1$ leads to the emergence of this new branch. While for $g = 0.028$ and $g = 0.03$ the branches A, B and C combine into one smooth curve, this is no longer true for $g = 0.032$, where the smooth curve is split into two at $gV_\infty = 1$. Hence for $g = 0.032$ branch C is disconnected from the branches A and B and a gap of values in $\phi(r_h)$ appears such that for these values no dyonic black holes with scalar hair exist.

5   Conclusions

In this paper, we have studied static, spherically symmetric black hole solutions that possess non-trivial scalar hair. These solutions exist in a complex scalar field model when coupled minimally to a U(1) gauge field. Next to electrically charged black holes, we have also discussed black holes with electric and magnetic charge. This is possible in a U(1) gauge theory since the source of the magnetic field is hidden behind the event horizon of the black hole. In comparison to a previous study done in [14], we have used a scalar field potential that is exponential in nature and hence bounded. Moreover, we have put the emphasis on studying the influence of the gauge coupling constant g, in particular for the cases of fixed background black hole solutions. We have also tried to directly compare the electric and the dyonic case. We find that the presence of the magnetic charge leads to some interesting qualitative features. Dyonic Reissner-Nordström black holes cannot carry arbitrarily large values of the scalar field on the horizon, while there is no upper limit on $\phi(r_h)$ for electrically charged Reissner-Nordström black holes. Moreover, we find that dyonic black holes can carry scalar fields that are actually very small on the horizon, something that is not possible for the purely electrically charged black holes.

13

References

[1] M. Heusler, *A No hair theorem for selfgravitating nonlinear sigma models*, J. Math. Phys. **33** (1992) 3497; J. D. Bekenstein, *Novel no-scalar-hair theorem for black holes*, Phys. Rev. D **51** (1995) no.12, R6608; D. Sudarsky, *A Simple proof of a no hair theorem in Einstein Higgs theory*, Class. Quant. Grav. **12** (1995) 579; T. Zannias, *Black holes cannot support conformal scalar hair*, J. Math. Phys. **36** (1995) 6970.

[2] H. Luckock and I. Moss, Black holes with Skyrmion hair, Phys. Lett. B **176** (1986), 341.

[3] P. Breitenlohner, P. Forgacs and D. Maison, Gravitating monopole solutions, Nucl. Phys. B **383** (1992), 357.

[4] T. H. R. Skyrme, A Nonlinear field theory, Proc. Roy. Soc. Lond. A **260** (1961), 127.

[5] G. 't Hooft, Magnetic Monopoles in Unified Gauge Theories, Nucl. Phys. B **79** (1974), 276.

[6] A. M. Polyakov, Particle Spectrum in the Quantum Field Theory, JETP Letters. **20** (1974), 194.

[7] D. J. Kaup, *Klein-Gordon Geon*, Phys. Rev. **172** (1968), 1331; R. Friedberg, T. D. Lee and Y. Pang, *Scalar Soliton Stars and Black Holes*, Phys. Rev. D **35** (1987), 3658.; P. Jetzer, *Boson stars*, Phys. Rept. **220** (1992), 163; A. R. Liddle, M. S. Madsen, *The Structure and formation of boson stars*, Int. J. Mod. Phys. D **1** (1992) 101

[8] F. E. Schunck and E. Mielke, *Rotating boson star as an effective mass torus in general relativity*, Phys. Lett. A **249** (1998), 389; E. Mielke and F. E. Schunck, *Boson stars: Rotation, formation, and evolution*, Gen. Rel. Grav. **31** (1999) 787; B. Kleihaus, J. Kunz and M. List, *Rotating boson stars and Q-balls*, Phys. Rev. D **72** (2005) 064002; B. Kleihaus, J. Kunz, M. List and I. Schaffer, *Rotating Boson Stars and Q-Balls. II. Negative Parity and Ergoregions*, Phys. Rev. D **77** (2008) 064025.

[9] I. Pena and D. Sudarsky, Do collapsed boson stars result in new types of black holes?, Class. Quant. Grav. **14** (1997), 3131.

[10] C. A. R. Herdeiro and E. Radu, *Kerr black holes with scalar hair*, Phys. Rev. Lett. **112** (2014) 221101; *Asymptotically flat black holes with scalar hair: a review*, Int. J. Mod. Phys. D **24** (2015) no.09, 1542014.

[11] J. P. Hong, M. Suzuki and M. Yamada, Spherically Symmetric Scalar Hair for Charged Black Holes, Phys. Rev. Lett. **125** (2020) no.11, 111104

[12] C. A. R. Herdeiro and E. Radu, Spherical electro-vacuum black holes with resonant, scalar Q-hair, Eur. Phys. J. C **80** (2020) no.5, 390

[13] Y. Brihaye and B. Hartmann, Strong gravity effects of charged Q-clouds and inflating black holes, Class. Quant. Grav. **38** (2021) no.6, 06LT01

[14] C. Herdeiro, E. Radu and Y. Shnir: Reissner-Nordström dyonic black holes with gauged scalar hair, Phys. Lett. B **856** (2024), 138912

[15] P. A. M. Dirac, Quantised singularities in the electromagnetic field, Proc. Roy. Soc. Lond. A, **133** (1931) 60–72

[16] Y. Brihaye, F. Cônsole and B. Hartmann: Inflation inside non-topological defects and scalar black holes, Symmetry **13** (2020) no.1, 2

[17] Y. Brihaye and B. Hartmann: Spherically symmetric charged black holes with wavy scalar hair, Class. Quant. Grav. **39** (2022) no.1, 015010

[18] Y. Brihaye and B. Hartmann: Boson stars and black holes with wavy scalar hair, Phys. Rev. D **105** (2022) no.10, 104063